Macromolecules
ARTICLE

Macromolecules **2010**, *43*, 9071–9076 **9071**
DOI: 10.1021/ma101990e

Hierarchical Smectic Self-Assembly of an ABC Miktoarm Star Terpolymer with a Helical Polypeptide Arm

Susanna Junnila,[†] Nikolay Houbenov,[†] Sirkku Hanski,[†] Hermis Iatrou,[‡] Akira Hirao,[§] Nikos Hadjichristidis,*[,‡] and Olli Ikkala*[,†]

[†]*Molecular Materials, Department of Applied Physics, Aalto University School of Science and Technology (previously Helsinki University of Technology), P.O. Box 15100, 00076 Aalto, Finland,* [‡]*Department of Chemistry, University of Athens, Panepistimiopolis, Zografou, 15771 Athens, Greece, and* [§]*Polymeric and Organic Materials Department, Graduate School of Science and Engineering, Tokyo Institute of Technology, Tokyo 152-8552, Japan*

Received August 27, 2010; Revised Manuscript Received October 1, 2010

ABSTRACT: We demonstrate the first hierarchical smectic self-assembly in miktoarm star terpolymers, using a polymer/polypeptide hybrid (macromolecular *chimera*) composed of two coil-like arms (polystyrene, PS, and polyisoprene, PI) and a mesogenic α-helical polypeptide arm (poly(ε-*tert*-butyloxycarbonyl-L-lysine), PBLL). The PBLL α-helices are packed within lamellar nanodomains which leads to an overall smectic alteration of rod- and coil-containing layers typically observed in rod−coil block copolymers. Furthermore, the coil-containing lamellae have an inner structure composed of PS and PI rectangular cylinders, leading to what we call a hierarchical smectic phase. To elucidate the role of polypeptide helices in directing the self-assembly, the ordering is studied both after thermal annealing and after quick drop-casting from chloroform solution. The possibility to combine mesogen packing, tiling patterns, and conformational control of polypeptide blocks makes self-assembled hierarchies of star-shaped macromolecular *chimeras* appealing for future studies.

Introduction

Self-assembly of block copolymers has been a powerful tool to create nanostructured materials for decades.[1,2] Beyond the classic linear AB diblock copolymers, many strategies have been introduced to achieve more complex block copolymer self-assemblies. The addition of a third block in a linear fashion leads to ABC-type block copolymers where there are three tunable interaction parameters (χ_{AB}, χ_{BC}, χ_{AC}), two independently controlled relative sizes of blocks ($f_A, f_B, f_C = 1 - f_A - f_B$), and three possible ways to combine the blocks (ABC, BAC, ACB), increasing the number of accessible self-assembled morphologies radically.[3,4] Following the same idea, even more blocks can be joined end-to-end to create so-called multiblock copolymers.[5,6] To extend the scope of achievable morphologies, nonlinear block copolymer architectures have attracted considerable interest.[7] In miktoarm star block copolymers,[8] specifically, multiple blocks are connected at a single branching point to form a star-shaped molecule with chemical asymmetry. The effects of this molecular architecture have been studied regarding, for example, lamellar spacing,[9] crystallization,[10,11] micellization in miktoarm/homopolymer blends,[12] and formation of polymersomes,[13] and multicompartment micelles.[14]

The synthesis[15,16] and self-assembly[17,18] of miktoarm star block copolymers have been studied prevalently in systems with three coil-like arms. Of these, the A_2B arrangement behaves essentially as an AB diblock copolymer with shifted phase boundaries due to the increased curvature at the interface of the blocks.[19,20] The ABC terpolymer architecture incorporating three chemically distinct coil-like arms is even more interesting.[4] When the three blocks are comparable in size, the miktoarms tend to self-assemble in 2D ordered structures consisting of cylinders with polygonal cross sections.[17,18,21] In these so-called tiling patterns, the branching points of the molecules are confined to lines in 3D space. Interestingly, also quasi-crystalline[22] and concentric columnar[23] tiling patterns have been observed. On the other hand, when one of the blocks is much longer than the other two, polygonal tiling patterns are no longer obtained. In this case, the longest block stabilizes in lamellar layers while the shorter two form alternating rectangular cylinders between the large-block lamellae.[24]

When one or more of the blocks are not coil-like, new packing frustration is introduced.[25,26] Even in the oligomeric case, so-called T-shaped ternary amphiphiles, i.e., rodlike mesogens equipped with both polar and nonpolar chains, lead to very complex self-assemblies.[27] When polypeptides are used in self-assemblies, conformations such as α-helices and β-sheets can be accessed.[28−32] In particular, the α-helical conformation leads to mesogenic rods which possess dipole moments, potentially include kinks, and have been extensively employed in polymer/polypeptide hybrid systems.[33−37] The conformational asymmetry of the blocks and the liquid crystalline packing tendency of the α-helical rods lead to predominantly lamellar[33] or ribbonlike[38] structures in the case of linear rod−coil block copolymers. An ABC miktoarm star terpolymer with an α-helical polypeptide block (poly(γ-benzyl-L-glutamate), PBLG) and two different coil-like blocks (PS, PI) has been reported to show microphase separation of PBLG from the PS and PI blocks.[39] However, well-defined hierarchies in polypeptide-containing miktoarms have so far been limited to the A_2B and AB_2 architectures which demonstrate microphase separation and helical packing resembling linear rod−coil block copolymers.[40,41]

We show for the first time formation of a well-ordered hierarchical self-assembly in an ABC miktoarm star terpolymer consisting of two amorphous coil-like polymer arms (PS, PI) and

*Corresponding authors. E-mail: olli.ikkala@tkk.fi (O.I.), hadjichristidis@chem.uoa.gr (N.H.).

Published on Web 10/14/2010

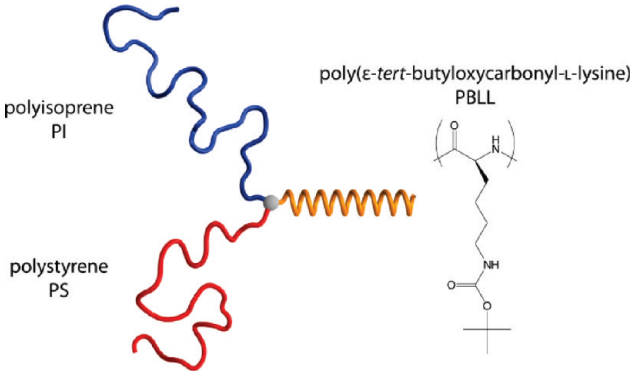

Figure 1. Schematic illustration of the (PS)(PI)(PBLL) miktoarm star terpolymer.

an α-helical polypeptide arm (PBLL). Structural and conformational analysis of the (PS)(PI)(PBLL) miktoarm is performed by transmission electron microscopy (TEM), atomic force microscopy (AFM), small- and wide-angle X-ray scattering (SAXS, WAXS), and Fourier transform infrared spectroscopy (FTIR).

Experimental Section

Synthesis. The synthesis of (PS)(PI)(PBLL) has been reported previously[42] and includes the preparation of a PS-NH_2-PI precursor where M_n(PS) = 10 000 g/mol and M_n(PI) = 13 000 g/mol (by SEC in THF at 40 °C) by anionic polymerization high-vacuum techniques and appropriate linking chemistry, followed by ring-opening polymerization of ε-*tert*-butyloxycarbonyl-L-lysine *N*-carboxyanhydride using the PS-NH_2-PI as a macroinitiator. The final total M_n(miktoarm) = 34 200 g/mol and M_w/M_n = 1.07 (by SEC-TALLS in DMF (0.1 N LiBr) at 60 °C). The wt % composition of the PS, PI, and PBLL arms is 30.1, 38.6, and 31.3, respectively (by ^{1}H NMR in $CDCl_3$). A schematic illustration of the molecule is shown in Figure 1.

Sample Preparation. (PS)(PI)(PBLL) was dissolved as 1 wt % solution in chloroform ($CHCl_3$, Sigma-Aldrich, ≥99.0%). The solubility parameters δ/(MPa)$^{1/2}$ are as follows: $CHCl_3$ 19.0; PS 17.4−19.0; PI 16.2−20.5; and PBLL 23.7 (values from the literature[43,44] except δ_{PBLL} estimated with Hoy Solubility Parameter Calculator by Computer Chemistry Consultancy). Samples were prepared in two ways: (1) drop-casting, i.e., evaporating the sample rapidly from $CHCl_3$ solution, followed by vacuum drying ($p < 10^{-2}$ mbar) to remove the remaining solvent, and (2) slow evaporation of $CHCl_3$ followed by vacuum drying ($p < 10^{-2}$ mbar) and thermal annealing of the bulk sample at 130 °C in vacuum ($p < 10^{-5}$ mbar) for 16 h.

TEM Characterization. Drop-cast samples were evaporated directly on lacey carbon support film grids placed on top of a filter paper and subsequently vacuum-dried. Annealed bulk samples were sectioned at −100 °C using a Leica Ultracut UCT ultramicrotome and a 25° Diatome diamond knife. Sections with a thickness of ca. 70 nm were collected on lacey carbon support film grids. The samples were stained at room temperature by exposing the grids to osmium tetroxide (OsO_4, 10 min) or ruthenium tetroxide (RuO_4, 1 min) vapors. Bright-field TEM was performed on a FEI Tecnai 12 transmission electron microscope operating at an accelerating voltage of 120 kV, and the images were recorded with a Gatan UltraScan 1000 CCD camera.

AFM. The sample was drop-cast on a silicon wafer, vacuum-dried, and imaged with a Veeco Dimension 5000 scanning probe microscope with Nanoscope V controller (Digital Instruments, Inc.). Silicon AFM tips (NSC 15/AIBS, MikroMasch) coated with Al with a tip radius of 10 nm were used in tapping mode. Scanning was conducted with scanning rates of 0.8−1 Hz under variable loading conditions (hard and light tapping modes).

SAXS and WAXS Measurements. For the X-ray scattering studies, the samples were sealed between Mylar films. The SAXS measurements were performed with a rotating anode Bruker Microstar microfocus X-ray source (Cu Kα radiation, λ = 1.54 Å) with Montel parallel optics. The beam was further collimated with four sets of JJ X-ray four-blade slits, resulting in a beam area of about 1 mm × 1 mm at the sample position. Scattering intensities were measured using a Bruker AXS HI-STAR 2D area detector. The sample-to-detector distance was 209 cm.

The WAXS measurements were performed using the second part of the same X-ray source with Montel focusing optics (Incoatec GmbH), resulting in a beam area of about 0.8 mm × 0.8 mm at the sample position. The scattering intensities were measured with a Bruker AXS Vantec 2D area detector, and the sample-to-detector distance was 10 cm.

X-ray diffraction data were measured from nonoriented bulk samples and integrated over the whole detector area. Background was measured separately and subtracted from the data. The magnitude of the scattering vector is given by $q = (4\pi/\lambda) \sin\theta$, where 2θ is the scattering angle.

FTIR Measurements. FTIR spectra of the samples were recorded with a Nicolet 380 FT-IR spectrometer with the ATR technique. 64 spectra were averaged with 2 cm^{-1} resolution. The spectra have been ATR corrected and smoothed with EZ Omnic 7.2 software Automatic smooth, which uses the Savitzky−Golay algorithm.

Results and Discussion

To investigate the structure formation of the (PS)(PI)(PBLL) miktoarm *chimera* (see Figure 1) in the solid state, samples with two different preparation pathways are reported: (1) a drop-cast sample, rapidly evaporated from $CHCl_3$ solution and (2) a slowly evaporated and thermally annealed bulk sample. The former preparation method sheds light to the driving forces dominating the self-assembly, whereas the latter one probes the thermodynamic equilibrium morphology. The thermal annealing conditions are limited by the decomposition of the material, observed to start already below 200 °C (by thermogravimetric analysis, see the Supporting Information, Figure S1) and, on the other hand, by the glass transition of the PS block at 107 °C (by differential scanning calorimetry, see Supporting Information, Figure S2). In addition, cleaving of the *N*-*tert*-butyloxycarbonyl (Boc) group has been reported to take place above 150 °C.[45,46] These factors severely limit the usable range of thermal annealing conditions, and an annealing temperature of 130 °C was therefore chosen. However, according to nuclear magnetic resonance measurements (^{1}H NMR, see Supporting Information, Figures S3 and S4), 35% of the Boc protecting groups of PBLL are thermolytically removed during such annealing, leaving the $-(CH_2)_4NH_2$ lysine side chain in the polypeptide. Lower annealing temperatures or solvent annealing, on the other hand, did not lead to sufficient improvement in the order of the material. Importantly, as is shown below, removal of part of the Boc groups is not observed to influence the self-assembly of (PS)(PI)(PBLL).

To compare the two different preparation methods, the miktoarm samples were imaged with TEM (Figure 2). The bulk annealed sample, exposed to RuO_4 vapors, shows a lamellar structure with periodicity of 21−26 nm (Figure 2a), consisting of alternating PBLL layers (appearing light in the image) and layers containing both PS and PI blocks (dark). To further investigate the internal structure of the PS/PI lamellae, the PI blocks of another sample were selectively stained with OsO_4. After staining, alternating PI (dark) and PS (light) domains are observed in the PS/PI lamellae of the bulk annealed sample (Figure 2c). These domains are rectangular cylinders, viewed along the direction of the cylindrical axis in Figure 2c (for examples of sideways view, see Supporting Information, Figure S5). The repeating distance

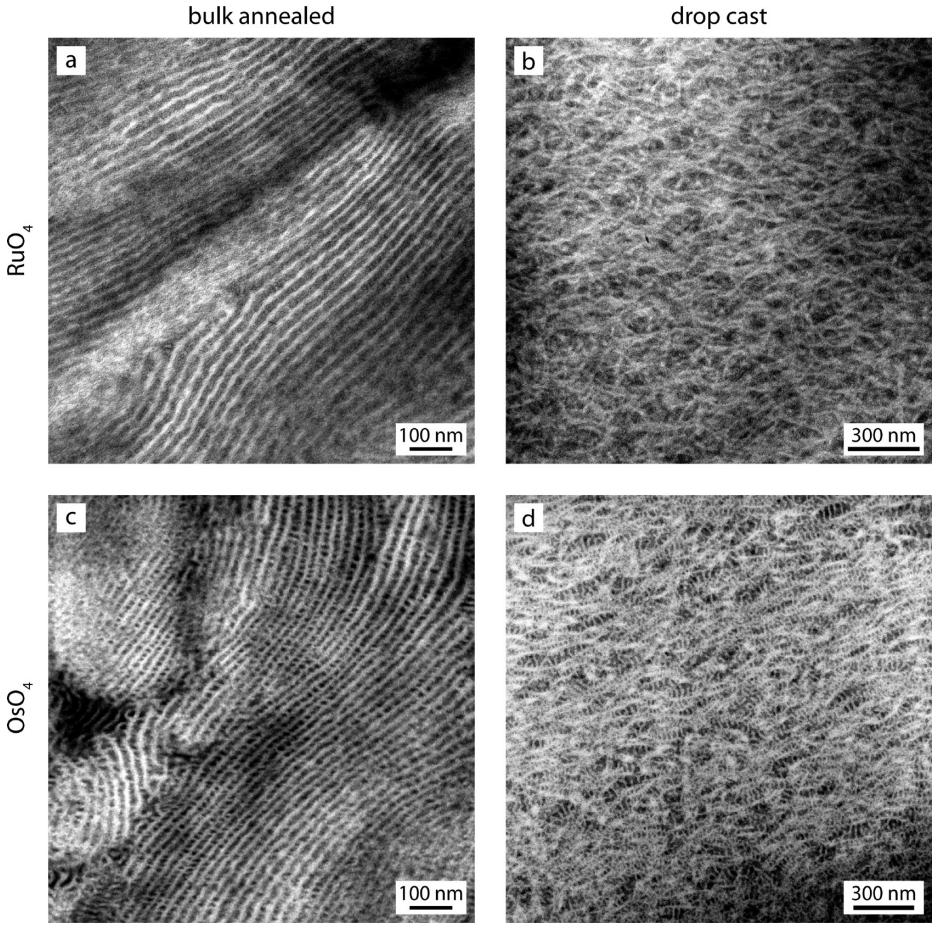

Figure 2. TEM micrographs of the miktoarm bulk annealed and drop-cast samples as stained with (a, b) RuO_4 (PS and PI dark, PBLL light) and (c, d) OsO_4 (PI dark, PS and PBLL light).

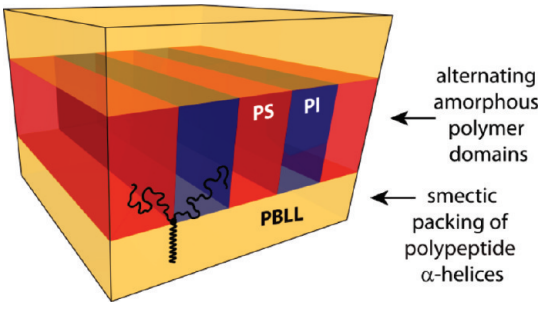

Figure 3. Schematic illustration of the self-assembly of the (PS)(PI)-(PBLL) miktoarm. PBLL conformation and packing are discussed in detail later.

between adjacent PI domains within a single layer is 14−19 nm. This two-level hierarchical structure is schematically shown in Figure 3.

In the rapidly prepared drop-cast sample, a relatively poor overall order is observed. However, also in this case lamellae are observed after RuO_4 staining (Figure 2b), although with less regular spacing and alignment. Upon OsO_4 staining of the PI domains (Figure 2d), a three-phase structure is revealed, where PBLL form extended lamellae with no overall alignment, separated by alternating PS/PI domains. In other words, a very similar arrangement of the molecules takes place on the local scale, even if the level of order is considerably lower than in the annealed sample.

The hierarchical structure is also found on the top surface of the sample, as witnessed by AFM phase contrast imaging (Figure 4).

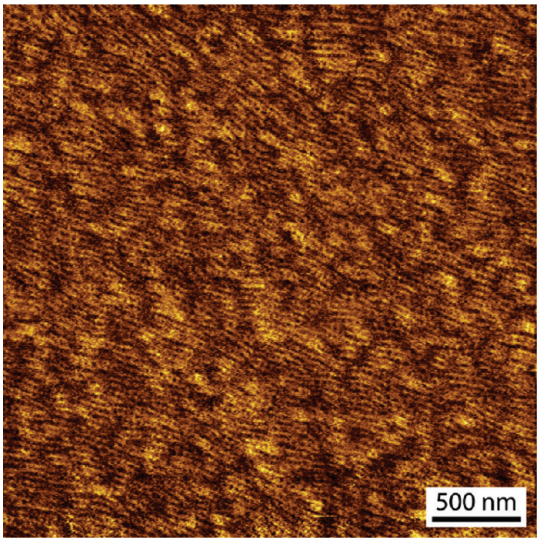

Figure 4. AFM phase contrast image of the miktoarm as drop-cast from $CHCl_3$ solution.

The phase contrast between the glassy PS (light) and the rubbery PI (dark) blocks is observed between the rigid PBLL lamellae (light).

To verify the structural sizes observed by TEM, X-ray scattering studies were performed. In spite of the annealing, the SAXS curve of the bulk sample lacks multiple sharp reflections and shows only a small shoulder at 0.024 $Å^{-1}$ (Figure 5). This corresponds to a size of 26 nm, which is in good agreement with

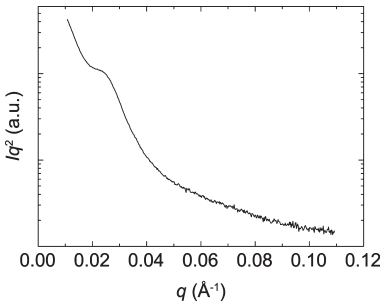

Figure 5. SAXS curve of the bulk annealed miktoarm demonstrates a shoulder at 0.024 $Å^{-1}$, corresponding to a size of 26 nm. The reflection is expected to originate from the repeating distance of the alternating PBLL and PS/PI lamellae.

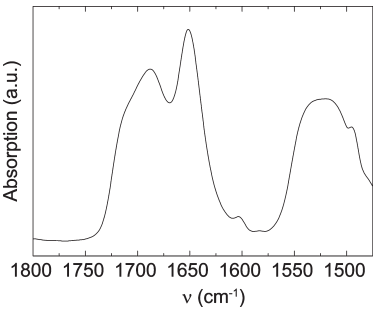

Figure 6. FTIR spectrum of the bulk annealed miktoarm shows an amide I absorption at 1650 cm^{-1}, typical for α-helical conformation.

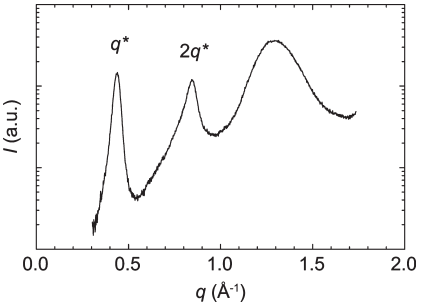

Figure 7. WAXS curve of the bulk annealed miktoarm. The reflections q^* and $2q^*$ demonstrate a well-ordered packing of the PBLL α-helices.

the repeating distance of the PBLL and PS/PI lamellae observed in TEM. A similar but slightly less intensive shoulder is observed in the drop-cast sample (see Supporting Information, Figure S6).

Next, the internal structure of the PBLL lamellae is discussed. The FTIR amide band region spectrum of the bulk annealed sample shows a clear amide I absorption at 1650 cm^{-1} (Figure 6). This absorption originates from the C═O stretching of the peptide linkage and corresponds to α-helical conformation. Because of overlapping peaks, the amide II region at 1560−1530 cm^{-1} cannot be reliably used in the conformational studies. In the drop-cast sample, a similar absorption is observed at 1649 cm^{-1}, also illustrating α-helical conformation (see Supporting Information, Figure S7). In other words, the PBLL arms are essentially rigid-rod-like mesogenic blocks, potentially including also kinks.

In the WAXS curve of the bulk annealed sample, two sharp reflections are observed at $q^* = 0.44$ $Å^{-1}$ and $2q^* = 0.85$ $Å^{-1}$ (Figure 7). These reflections indicate a well-ordered packing of the PBLL α-helices within the polypeptide layer. Between these reflections, evidence of increased scattering is observed, but the absence of explicit reflections especially at $\sqrt{2}q^*$ or $\sqrt{3}q^*$ unfortunately prohibits confirmation of whether the PBLL α-helices are packed in a hexagonal or tetragonal manner. Hexagonal packing has been reported in several polymer/polypeptide *chimeras*,[33,34,39] but arguments can be given also for the tetragonal lattice which enables perfect compensation of dipole moments in the case of interdigitating helices. In our case, the helix-to-helix distance would be 1.6 or 1.4 nm, assuming hexagonal or tetragonal packing, respectively, as calculated based on the location of the q^* reflection. Both values are reasonable, considering the chemical structure of PBLL. In addition, a broad reflection is observed at 1.29 $Å^{-1}$ which can be assigned to the average distance of amorphous segments, including styrene pendant groups of PS.[40] Similar but slightly broader reflections are observed in the drop-cast sample, corresponding to helix-to-helix distances of 1.7 or 1.5 nm for the hexagonal or tetragonal packing, respectively (see Supporting Information, Figure S8).

In conclusion, the (PS)(PI)(PBLL) miktoarm self-assembles in a hierarchical manner in a smectic lamellar superstructure where every other lamella is composed of PBLL α-helices and every other contains rectangular PS/PI cylinders (schematically shown in Figure 3). The local order appears to be similar both in the bulk annealed sample and the drop-cast sample, as shown by TEM, but the overall order is increased notably after thermal annealing. The poor long-distance order observed in the drop-cast sample is easily justified by the rapid evaporation conditions, which lead to kinetic trapping of the molecules and the subsequent self-assembly within a few seconds. Despite the two different preparation pathways—thermal annealing which leads to the thermodynamic equilibrium structure and rapid evaporation—similar stacking of the α-helical PBLL blocks is observed in both samples. This means that the packing of the helices takes place rapidly and is the main driving force for the formation of the hierarchical smectic self-assembly. It should be noted that in this kind of morphology the miktoarm branching points are no longer confined to 1D lines but can exist anywhere on the 2D lamellar interface.

These observations need to be considered in relation to two previous findings.

First, miktoarm star terpolymers with coil-like chains, i.e., without polypeptidic or rodlike mesogenic arms, form 2D tiling patterns consisting of polygonal cylinders when the arms are roughly of the same size.[17,24] A hierarchical structure composed of rectangular cylinders of A/B between C lamellae is observed experimentally only when the volume fractions of the arms are highly asymmetric: 1:1:x where $x = 3.0-4.9$.[24] Also in simulations, this hierarchical structure is demonstrated when the interactions between all of the arms are symmetrical (i.e., all χ are identical) and the volume fraction of one of the blocks is significantly (2−5 times) larger than the others.[47−50] If all three arms have symmetric volume fractions, asymmetric interaction parameters are required in the simulations for this hierarchical structure to form.[51] Experimentally, lamellar self-assembly with alternating rectangular cylinders has also been observed in blends of two diblock copolymers with mutual hydrogen bonding[52] and in linear multiblock terpolymers.[6] In our case, the packing tendency of the mesogenic α-helical PBLL blocks leads to the hierarchical smectic structure although this is not expected from the molecular weights of the arms (PS:PI:PBLL 1.0:1.3:1.0). In this sense, the (PS)(PI)(PBLL) system can be considered a miktoarm polymer analogue of linear rod−coil block copolymers[33] and even T-shaped liquid crystals[27] where self-assembly is influenced by the aggregation of rodlike moieties.

Second, the present work is the first time well-defined order and hierarchical smectic self-assembly is observed, while previous research on a corresponding material did not describe such structural hierarchy.[39] This reflects the challenges to identify suitable processing and annealing conditions in macromolecular *chimeras*, as provided in this work.

Next, we present simple geometric arguments for clarifying the helical packing in the direction perpendicular to the PBLL

lamellae. The helices can be organized in one of three ways: (1) tail-to-tail arrangement, leading to a bilayer of α-helices, (2) interdigitation of α-helices, or (3) folding of nonideal α-helices back and forth, i.e., rods having kinks and a reduced persistence length. In addition, tilting of the helices is possible. Unfortunately, TEM cannot be used to resolve the thicknesses of individual lamellae since both staining and focus play a major role here, enabling reliable extraction of the total lamellar period only. However, it is known that PBLL constitutes only 31.3 wt % of the miktoarm and that the length of a single ideal PBLL α-helix would be 7.0 nm, as calculated based on the molecular weight of the PBLL arm (10 700 g/mol) and the known rise of 0.15 nm per monomer in an α-helix. Therefore, the tail-to-tail arrangement which would take up to 14 nm of space seems highly implausible within a total lamellar periodicity of only 26 nm (by SAXS), also as it does not allow compensation of the α-helix dipole moments. Folding of the chains, on the other hand, would reduce the thickness of the PBLL lamellae to be less than the length of an ideal helix,[33,35] lowering the density of the PS/PI phase to be unconvincingly low (as calculated based on lamellar periodicity of 26 nm, assuming once-folded helices in a hexagonal array with a helix-to-helix distance of 1.6 nm, for example). Also, poor hydrogen-bonding solvents, such as the $CHCl_3$ used in this study, have been reported to promote formation of more ideal helices.[53] Finally, interdigitation would lead to a thickness of the PBLL lamellae comparable to the length of an ideal helix, which is also close to the expected ratio of lamellar thicknesses based on the molecular weights of the arms. Interdigitation also allows antiparallel arrangement of the α-helices. According to the above arguments, our hypothesis is that the factor controlling the self-assembled pattern is the interdigitation of PBLL α-helices in an antiparallel manner.

Partial removal of the Boc groups during thermal annealing does not influence the self-assembly of (PS)(PI)(PBLL), as the conformation of the polypeptide is not changed (shown by FTIR), and similar reflections are observed due to helical packing in WAXS before and after annealing. This is plausible since the Boc groups are expected to cleave randomly throughout the whole sample, and most of the PBLL side chains are not at all affected by the annealing. Therefore, thermal annealing can be used to improve the ordering of the material, as observed by TEM and SAXS.

Conclusions

We report the first well-defined hierarchical self-assembly of a miktoarm star terpolymer with two coil-like arms and an α-helical mesogenic polypeptide arm in the solid state. After appropriate thermal annealing, the (PS)(PI)(PBLL) miktoarm forms a hierarchical smectic self-assembly where the α-helical rod-like PBLL blocks stack to form pure polypeptide lamellae while the PS and PI blocks form lamellae with an inner structure composed of rectangular cylinders. This morphology is also observed locally already after quick drop-casting from chloroform solution, indicating the powerful driving force of the α-helical stacking in the formation of the structure. We expect that star-shaped macromolecular *chimeras* can lead to new complex hierarchical self-assemblies, where the polypeptide conformation and the material properties can be tuned, and potentially even to Janus-type particles.

Acknowledgment. Panu Hiekkataipale is thanked for the practical help and discussions related to the X-ray measurements and Henna Rosilo for the NMR measurements as well as interpretation. The New Energy Technologies group and the Polymer Technology group at Aalto University are thanked for the use of TGA and DSC, respectively. The Academy of Finland and the Finnish Foundation for Technology Promotion are gratefully acknowledged for financial support.

Supporting Information Available: TGA, DSC, and ^1H NMR measurements, additional TEM image of the bulk annealed sample, and SAXS, FTIR, and WAXS measurements of the drop-cast sample. This material is available free of charge via the Internet at http://pubs.acs.org.

References and Notes

(1) Bates, F. S.; Fredrickson, G. H. *Annu. Rev. Phys. Chem.* **1990**, *41*, 525–557.
(2) Hamley, I. W. *The Physics of Block Copolymers*; Oxford University Press: New York, 1998; p 424.
(3) Bates, F. S.; Fredrickson, G. H. *Phys. Today* **1999**, *52* (2), 32–38.
(4) Hadjichristidis, N.; Iatrou, H.; Pitsikalis, M.; Pispas, S.; Avgeropoulos, A. *Prog. Polym. Sci.* **2005**, *30*, 725–782.
(5) Masuda, J.; Takano, A.; Nagata, Y.; Noro, A.; Matsushita, Y. *Phys. Rev. Lett.* **2006**, *97*, 098301.
(6) Fleury, G.; Bates, F. S. *Macromolecules* **2009**, *42*, 1691–1694.
(7) Pitsikalis, M.; Pispas, S.; Mays, J. W.; Hadjichristidis, N. *Adv. Polym. Sci.* **1998**, *135*, 1–137.
(8) Hadjichristidis, N. *J. Polym. Sci., Part A: Polym. Chem.* **1999**, *37*, 857–871.
(9) Zhu, Y. Q.; Gido, S. P.; Moshakou, M.; Iatrou, H.; Hadjichristidis, N.; Park, S.; Chang, T. *Macromolecules* **2003**, *36*, 5719–5724.
(10) Floudas, G.; Reiter, G.; Lambert, O.; Dumas, P. *Macromolecules* **1998**, *31*, 7279–7290.
(11) Lorenzo, A. T.; Muller, A. J.; Lin, M. C.; Chen, H. L.; Jeng, U. S.; Priftis, D.; Pitsikalis, M.; Hadjichristidis, N. *Macromolecules* **2009**, *42*, 8353–8364.
(12) Pavlopoulou, E.; Anastasiadis, S. H.; Iatrou, H.; Moshakou, M.; Hadjichristidis, N.; Portale, G.; Bras, W. *Macromolecules* **2009**, *42*, 5285–5295.
(13) Yin, H. Q.; Kang, S. W.; Bae, Y. H. *Macromolecules* **2009**, *42*, 7456–7464.
(14) Li, Z. B.; Kesselman, E.; Talmon, Y.; Hillmyer, M. A.; Lodge, T. P. *Science* **2004**, *306*, 98–101.
(15) Fujimoto, T.; Zhang, H. M.; Kazama, T.; Isono, Y.; Hasegawa, H.; Hashimoto, T. *Polymer* **1992**, *33*, 2208–2213.
(16) Iatrou, H.; Hadjichristidis, N. *Macromolecules* **1992**, *25*, 4649–4651.
(17) Sioula, S.; Hadjichristidis, N.; Thomas, E. L. *Macromolecules* **1998**, *31*, 8429–8432.
(18) Huckstadt, H.; Gopfert, A.; Abetz, V. *Macromol. Chem. Phys.* **2000**, *201*, 296–307.
(19) Hadjichristidis, N.; Iatrou, H.; Behal, S. K.; Chludzinski, J. J.; Disko, M. M.; Garner, R. T.; Liang, K. S.; Lohse, D. J.; Milner, S. T. *Macromolecules* **1993**, *26*, 5812–5815.
(20) Tselikas, Y.; Iatrou, H.; Hadjichristidis, N.; Liang, K. S.; Mohanty, K.; Lohse, D. J. *J. Chem. Phys.* **1996**, *105*, 2456–2462.
(21) Yamauchi, K.; Takahashi, K.; Hasegawa, H.; Iatrou, H.; Hadjichristidis, N.; Kaneko, T.; Nishikawa, Y.; Jinnai, H.; Matsui, T.; Nishioka, H.; Shimizu, M.; Fukukawa, H. *Macromolecules* **2003**, *36*, 6962–6966.
(22) Hayashida, K.; Dotera, T.; Takano, A.; Matsushita, Y. *Phys. Rev. Lett.* **2007**, *98*, 195502.
(23) Sioula, S.; Hadjichristidis, N.; Thomas, E. L. *Macromolecules* **1998**, *31*, 5272–5277.
(24) Takano, A.; Kawashima, W.; Wada, S.; Hayashida, K.; Sato, S.; Kawahara, S.; Isono, Y.; Makihara, M.; Tanaka, N.; Kawaguchi, D.; Matsushita, Y. *J. Polym. Sci., Part B: Polym. Phys.* **2007**, *45*, 2277–2283.
(25) Klok, H. A.; Lecommandoux, S. *Adv. Mater.* **2001**, *13*, 1217–1229.
(26) Lee, M.; Cho, B. K.; Zin, W. C. *Chem. Rev.* **2001**, *101*, 3869–3892.
(27) Tschierske, C. *Chem. Soc. Rev.* **2007**, *36*, 1930–1970.
(28) Watanabe, J.; Ono, H.; Uematsu, I.; Abe, A. *Macromolecules* **1985**, *18*, 2141–2148.
(29) Ponomarenko, E. A.; Tirrell, D. A.; MacKnight, W. J. *Macromolecules* **1996**, *29*, 8751–8758.
(30) Hanski, S.; Houbenov, N.; Ruokolainen, J.; Chondronicola, D.; Iatrou, H.; Hadjichristidis, N.; Ikkala, O. *Biomacromolecules* **2006**, *7*, 3379–3384.
(31) Hanski, S.; Junnila, S.; Almasy, L.; Ruokolainen, J.; Ikkala, O. *Macromolecules* **2008**, *41*, 866–872.

(32) Junnila, S.; Hanski, S.; Oakley, R. J.; Nummelin, S.; Ruokolainen, J.; Faul, C. F. J.; Ikkala, O. *Biomacromolecules* **2009**, *10*, 2787–2794.
(33) Douy, A.; Gallot, B. *Polymer* **1982**, *23*, 1039–1044.
(34) Klok, H. A.; Langenwalter, J. F.; Lecommandoux, S. *Macromolecules* **2000**, *33*, 7819–7826.
(35) Losik, M.; Kubowicz, S.; Smarsly, B.; Schlaad, H. *Eur. Phys. J. E* **2004**, *15*, 407–411.
(36) Schlaad, H.; Smarsly, B.; Losik, M. *Macromolecules* **2004**, *37*, 2210–2214.
(37) Sanchez-Ferrer, A.; Mezzenga, R. *Macromolecules* **2010**, *43*, 1093–1100.
(38) Deming, T. J. *Prog. Polym. Sci.* **2007**, *32*, 858–875.
(39) Gitsas, A.; Floudas, G.; Mondeshki, M.; Lieberwirth, I.; Spiess, H. W.; Iatrou, H.; Hadjichristidis, N.; Hirao, A. *Macromolecules* **2010**, *43*, 1874–1881.
(40) Babin, J.; Taton, D.; Brinkmann, M.; Lecommandoux, S. *Macromolecules* **2008**, *41*, 1384–1392.
(41) Sun, J.; Chen, X. S.; Guo, J. S.; Shi, Q.; Xie, Z. G.; Jing, X. B. *Polymer* **2009**, *50*, 455–461.
(42) Karatzas, A.; Iatrou, H.; Hadjichristidis, N.; Inoue, K.; Sugiyama, K.; Hirao, A. *Biomacromolecules* **2008**, *9*, 2072–2080.
(43) Grulke, E. A. In *Polymer Handbook*, 3rd ed.; Brandrup, J., Immergut, E. H., Eds.; John Wiley & Sons: New York, 1989; p 1904.
(44) Krevelen, D. W. v. *Properties of Polymers*, 3rd ed.; Elsevier: Amsterdam, 1990; p 875.
(45) Rawal, V. H.; Cava, M. P. *Tetrahedron Lett.* **1985**, *26*, 6141–6142.
(46) Rawal, V. H.; Jones, R. J.; Cava, M. P. *J. Org. Chem.* **1987**, *52*, 19–28.
(47) Gemma, T.; Hatano, A.; Dotera, T. *Macromolecules* **2002**, *35*, 3225–3237.
(48) Tang, P.; Qiu, F.; Zhang, H. D.; Yang, Y. L. *J. Phys. Chem. B* **2004**, *108*, 8434–8438.
(49) Xu, Y. C.; Li, W. H.; Qiu, F.; Zhang, H. D.; Yang, Y. L.; Shi, A. C. *J. Polym. Sci., Part B: Polym. Phys.* **2010**, *48*, 1101–1109.
(50) Zhang, G. J.; Qiu, F.; Zhang, H. D.; Yang, Y. L.; Shi, A. C. *Macromolecules* **2010**, *43*, 2981–2989.
(51) Bohbot-Raviv, Y.; Wang, Z. G. *Phys. Rev. Lett.* **2000**, *85*, 3428–3431.
(52) Asari, T.; Matsuo, S.; Takano, A.; Matsushita, Y. *Macromolecules* **2005**, *38*, 8811–8815.
(53) Schlaad, H.; Smarsly, B.; Below, I. *Macromolecules* **2006**, *39*, 4631–4632.